ANALYSIS OF FLOW-INDUCED VIBRATIONS OF A SLIDE GATE CHAIN USING MONOLITHIC FLUID-STRUCTURE COUPLING

Björn Hübner, Ulrich Seidel, Jiri Koutnik

Voith Siemens Hydro Power Generation GmbH & Co. KG
Alexanderstraße 11, 89522 Heidenheim, Germany
bjoern.huebner@vs-hydro.com, ulrich.seidel@vs-hydro.com, jiri.koutnik@vs-hydro.com

ABSTRACT

During operation of a bottom outlet with a closed slide gate and an opend roller-mounted gate, a high velocity water flow (up to 80 m/s) occurs in the duct of the slide gate chain. The flow induces large amplidude chain vibrations perpendicular to the broadside of chain elements.

In order to investigate the excitation mechanism and to compare different cross-sectional shapes of the lifting device by means of numerical simulation, a simplified model is developed. The chain is placed in the center of a square channel and modeled as a continuous plate structure with reduced stiffness to account for joints between the elements. For numerical simulation, a monolithic coupling of Navier-Stokes fluid dynamics and non-linear structural dynamics applies. The calculation model is based on a unified space-time finite element method. Stability limits of the simplified chain structure are identified by means of transient simulations with slowly increasing inflow velocity.

In addition to the chain model with rectangular cross-section, also a cable with circular cross-section, equal axial stiffnes, and low bending stiffness is regarded, leading to a stability limit at higher inflow velocities. Thus, by using a cable instead of a chain for slide gate operation, the situation may be improve, but high amplitude flow induced vibrations cannot be prevented completely.

1. INTRODUCTION

In most freshwater reservoirs, a bottom outlet is designed to empty the reservoir for maintenance reasons. At high watermarks and the danger of a dam overflow, it may also be used as an emergency outlet. The present paper regards a bottom outlet in which a slide gate and a roller-mounted gate are arranged subsequently. During normal outlet operation, the slide gate is closed, and the roller-mounted gate starts to open. Now, the water is flowing 11 meters in upward direction through the slide gate duct before it is flowing back in an additional duct and passing the roller-mounted gate. When the roller-mounted gate is half opened, the water flow inside the slide gate duct reaches a certain but not exactly known velocity which induces high amplitude vibrations of the slide gate chain perpendicular to the broadside of chain elements. The unstable system behavior remains when the roller-mounted gate is fully opened. In this case, a flow velocity of approx. 80 m/s has been measured in the slide gate chain duct. Figure 1 shows a view into the duct including the chain. The overall length of the duct is 50 meters, but only the lower 11 meters are filled with water.

Figure 1: View into the duct of the slide gate chain.

Goal of this work is to study the excitation mechanism and to compare stability limits of chains and cables with different cross-sectional shapes to find an improved solution for the slide gate lifting device.

For this purpose, a simplified model of the coupled system suitable for numerical simulations is developed and described in section 3. Previously, the numerical solution procedure for analyzing strongly coupled fluid-structure interaction is summarized in section 2. Numerical results for a chain like structure with rectangular cross-section and an alternative cable structure with circular cross-section and very low bending stiffness are compared in section 4.

2. NUMERICAL SOLUTION PROCEDURE

For the numerical simulation of the coupled system in time domain, a monolithic coupling of incompressible Navier-Stokes fluid dynamics and geometrically non-linear structural dynamics applies. The solution procedure is based on a unified space-time finite element method which is described in detail by Hübner et al. (2004). Hübner and Dinkler (2005) apply the methodology to identify hydroelastic instabilities of a fluid-conveying cantilevered pipe system which is defined and experimentally investigated by Païdoussis and Semler (1998).

The governing equations for both solid and fluid are formulated in velocity variables and discretized with stabilized and time-discontinuous space-time finite elements. A continuous finite element mesh applies to the entire spatial domain. Therefore, the velocity variables at the interface belong to both fluid and structural domain fulfilling the coupling conditions automatically. The discretized model equations are assembled altogether in a single set of algebraic equations, considering the two-field problem as a whole.

The space-time finite element method provides a consistent discretization of both space and time, avoiding semi-discrete formulations. Using isoparametric space-time elements, which are adaptable in time direction, the method discretizes model equations in moving domains in a natural way and satisfies inherently the geometric conservation law. At discrete time levels, the interpolation of velocity, stress and pressure variables is discontinuous in time using independent degrees of freedom for the values at the end of the previous and at the beginning of the actual time slab. This time-discontinuous Galerkin formulation results in a fully implicit time integration scheme which is A-stable and of third-order accurate. A Petrov-Galerkin stabilization of space-time elements prevents numerical oscillations in case of convection dominated flows and allows the application of interpolation functions of equal order for velocities and pressure. The mixed-hybrid velocity-stress formulation of structural elements prevents all kinds of locking effects.

The highly nonlinear system of discretized model equations for solid, fluid, and fluid mesh dynamics has to be solved iteratively. Due to the application of a continuous finite element mesh for the entire domain, a monolithic formulation of solid and fluid in a single system of algebraic equations is obtained. A Picard iteration scheme linearizes all equations, leading to a relatively simple fixed point type solution procedure. Thus, the entire set of model equations for solid, fluid, and fluid mesh dynamics is solved in a single iteration loop. In case of strong structural nonlinearities, the iteration is accelerated by applying a relaxation scheme for the calculation of structural displacements. For the relaxation parameter, values between 0.7 and 1.0 are appropriate in most cases.

For solving the large sparse system of linearized equations, a preconditioned BiCGStab solver is used. However, a major difficulty is the choice of appropriate preconditioning methods. The matrix is not diagonally dominant and may be ill-conditioned if different scales are present in fluid and structure. Therefore, a direct LU-factorization of the system matrix is used for preconditioning during a variable number of time steps. When system characteristics change significantly, the system matrix has to be factorized again.

3. MODELING OF CHAIN AND CABLE STRUCTURE IN AXIAL FLOW

In order to investigate flow induced vibrations and to find an improved design for the slide gate lifting device, the existing chain structure is compared with a cable model. A clear advantage of the cable is the non-existence of bolt connections which therefore cannot be destroyed by large amplitude vibrations, but the bending stiffness is much smaller and may lead to a lower stability limit or higher amplitudes. However, the contact surface for the flow is smaller and the flow around the vibrating cable is more complex. Therefore, a simplified model of the coupled system suitable for efficient numerical analyses is regarded to compare stability characteristics of chain and cable structure. Both lifting devices are placed in the center of a water filled quadratic channel, see figure 2, and modeled as elastic solids with adapted stiffness properties to approximately account for the real structural behavior.

3.1 Channel flow

For the flow simulation, an incompressible and viscous fluid including buoyancy effects is assumed and described by the instationary Navier-Stokes equations. At the lower end of the channel (inlet), a slowly increasing inflow velocity is imposed by $v(t) = 40\ \text{m/s} + t \cdot 0.5\ \text{m/s}^2$. At the upper end of the channel (outlet) zero pressure boundary conditions apply, see figure 2. With a density of $\rho = 1.0\ \text{t/m}^3$ and a viscosity of $\mu = 1 \cdot 10^{-6}\ \text{t/(m s)}$ the Reynolds number based on the channel width is $Re = 4 \cdot 10^7$ for a flow velocity of 40 m/s. Thus, the flow field is clearly turbulent. However, turbulence modeling does not apply since the coarse fluid mesh, which is necessary for solving the coupled system over a large period with a small time step of $\Delta t = 0.005$ s, cannot resolve turbulent boundary layer flows. Therefore, slip boundary conditions apply at the

channel walls. At the fluid-structure interface no-slip conditions are present, and the boundary layer thickness is mainly defined by the thickness of the first element layer. In order to investigate the influence of viscosity and boundary layer effects on stability limits of the coupled system, the viscosity is 10-fold increased, and the results are compared to the original case.

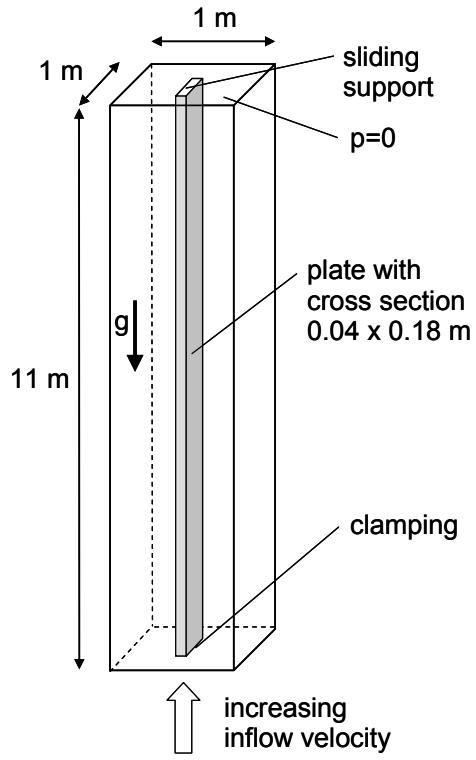

Figure 2: System configuration of simplified model.

3.2 Chain with rectangular cross-section

The original chain is modeled as a beam like plate structure with rectangular cross-section and discretized with 3-dimensional solid elements for geometrically non-linear elastodynamics. From the entire chain, only the lower part which is immersed in water is regarded. At the upper end where the chain is cut off, a sliding support with fixed rotation applies, and at the lower end where the slide gate is attached, a clamping is placed. To account for the joints between chain elements, Young's modulus of the elastic solid, given by $E = 1 \cdot 10^8$ kN/m^2, is reduced to approximately half the value of steel. However, keep in mind, that also the real chain has a finite bending stiffness against deflections perpendicular to the broadside. For density and dead load, the real values of steel of $\rho = 7.8$ t/m^3 and $\gamma = 78$ kN/m^3 apply. Beside the damping due to the viscous fluid, only a very small volume proportional damping coefficient of $b = 0.01$ t/(m^{3}s) acts on the structure. The system configuration with all dimensions of the simplified chain model is given in figure 2. For numerical analyses, symmetry is considered to reduce the model size, see finite element mesh of a cross-sectional plane in figure 3.

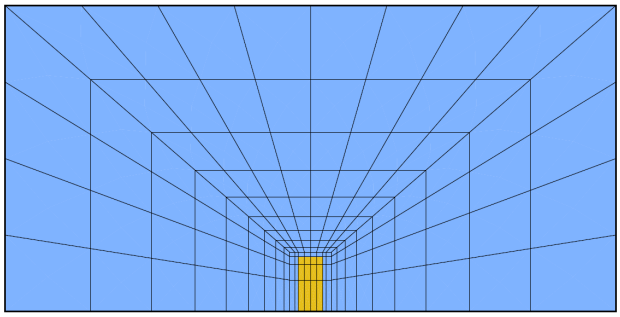

Figure 3: Cross-sectional mesh for the chain.

3.3 Cable with circular cross-section

Also for the alternative cable structure, symmetry conditions apply, and only half of the model is discretized, see the finite element mesh of a cross-sectional plane given in figure 4. However, this restricts the solution to in-plane vibration modes, even though three-dimensional vibration shapes are quite possible in case of circular cables. Upper and lower boundary conditions as well as the coupling to the fluid domain are equal to the numerical model of the chain structure. The cable diameter of $D = 0.09$ m is chosen to match approximately the cross-sectional area of the chain model. In order to model real cable behavior exhibiting high axial stiffness and very low bending stiffness with an elastic solid, different Young's moduli are used in the center and at the outer regions of the cross-section. For the two elements in the center of the symmetric mesh, a value of $E_i = 1.26 \cdot 10^9$ kN/m^2 applies. For the outer elements, a much smaller value of $E_o = 1 \cdot 10^7$ kN/m^2 is used. Now, the axial stiffness of $EA = 7.2 \cdot 10^5$ kN is equal to the chain model, and the bending stiffness of $EJ = 65$ kNm^2 is clearly smaller. The values for density, dead load and damping are taken from the chain model.

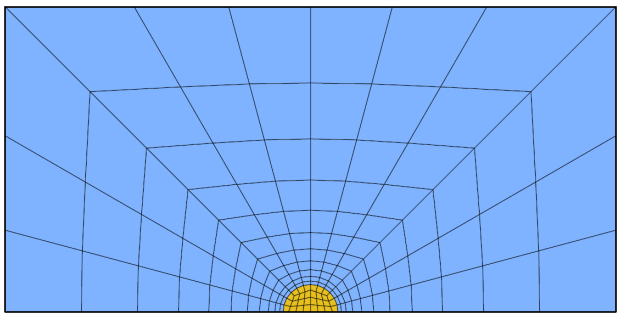

Figure 4: Cross-sectional mesh for the cable.

4. COMPARISON AND EVALUATION OF RESULTS

The simplified numerical model of the coupled system may not describe exactly the real physics of chain and cable structure in the turbulent flow field of the slide gate duct. However, the simplifications are comparable for both cases, and therefore, the numerical results allow a qualitative comparison of the sensitivity to flow induced vibrations and hydroelastic instabilities.

In order to determine the limit velocity for the occurrence of an hydroelastic instability leading to large amplitude vibrations, a horizontal impulse load is acting every 15 seconds on the upper end of the structure, while the inflow velocity is increasing continuously. The first impulse load acts after one seceond of calculation time when a stationary flow field and an equilibrium state of the structure is developed. The stability limit is reached at the point in time where the vibration amplitudes due to the impulse load start to increase.

When the first impulse load acts at 40.5 m/s inflow velocity on the original chain model, the structure responds initially with a damped vibration behavior. However, after 5.6 seconds of simulation time at v = 42.8 m/s inflow velocity, the dynamic behavior changes and the system gets unstable. See figure 5, where time histories of horizontal displacements at center and upper end of the chain model are shown for the first 12 seconds of simulation time. The vibration frequency which is increasing continuously with the inflow velocity, becomes f = 1.4 Hz at the stability limit.

The chain model with 10-fold increased fluid viscosity exhibits nearly identical stability characteristics. The stability limit is reached at a flow velocity of v = 43.2 m/s, and the corresponding frequency is given by f = 1.4 Hz, too, see time histories of displacements for the entire calculation time in figure 6. Thus, it can be concluded that boundary layer effects have only minor influence on the stability characteristics which are mainly influenced by inertia and convective effects. Snap shots of the deformed chain structure during a single period of the coupled vibration are shown in figure 8 for the case with 10-fold increased fluid viscosity. The type of motion can be classified as a kind of travelling wave flutter, similar to a flag in wind flow.

In case of the cable structure, the impulse load induces much larger initial deflections in the stable regime since bending stiffness and flow resistance are clearly smaller. Nevertheless, the vibrations due to the first impulse load decrease nearly to zero, and the hydroelastic instability occurs much later. At v = 50.0 m/s inflow velocity, the cable system tends to get unstable, but the amplitudes increase only slightly. The real stability limit exhibiting strongly increasing amplitudes is first reached at an inflow velocity of v = 60.2 m/s, see time histories of displacements in figure 7. Stability limits and corresponding frequencies of all regarded models are compared in table 1.

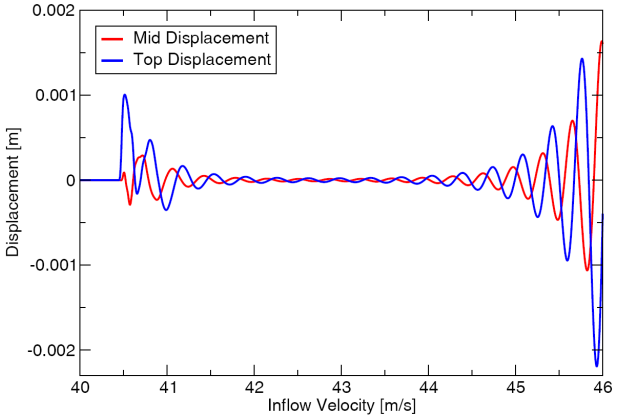

Figure 5: Time history of horizontal displacements near to the satbility limit for the chain model.

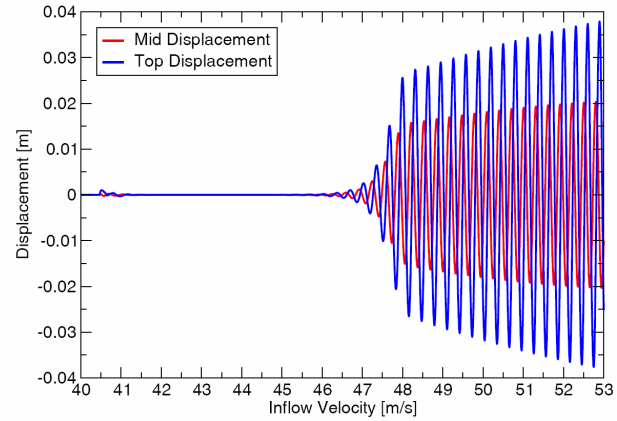

Figure 6: Time history of horizontal displacements for the chain model with 10-fold fluid viscosity.

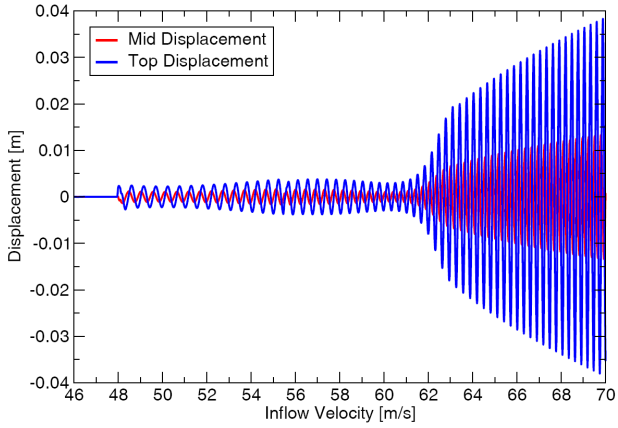

Figure 7: Time history of horizontal displacements after second impulse load for the cable model.

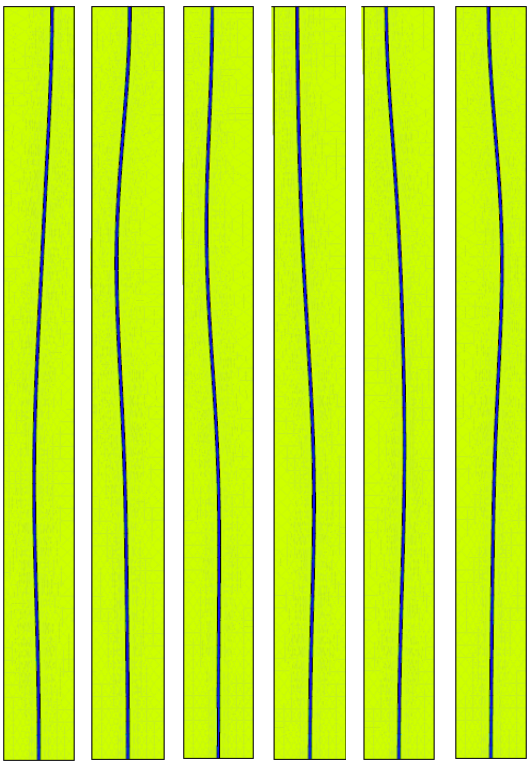

Figure 8: Snap shots of deformed chain structure (5-times magnified) during coupled vibration.

model	flow velocity at stability limit	corresponding frequency
rectangular chain	42.8 m/s	1.4 Hz
chain (10-fold visc.)	43.2 m/s	1.4 Hz
circular cable (1st)	50.0 m/s	1.9 Hz
circular cable (2nd)	60.2 m/s	2.8 Hz

Table 1: Stability limits of chain and cable.

Although the bending stiffness of the cable model is clearly smaller compared to the chain model, instability occurs at much higher flow velocities. This behavior is caused by the different cross-sectional shapes leading to different flow situations. In case of the chain model, the flow is syncronized over the entire contact surface (broadside of the chain) leading to approximately two-dimensional flow behavior. In contrast, the contact surface of the cable model is clearly smaller and the circular shape causes a fully 3-dimensional and more complex flow situation. This results in the favorable stability characteristics of the cable model, at least if only in-plane vibrations are regarded. However, for both lifting devices, large amplitude flow induced vibrations have been detected within the operating range of up to 80 m/s flow velocity. Nevertheless, the cable seems to have clear advantages over the chain structure.

5. CONCLUSION

In order to find reasons for large amplitude flow induced vibrations of a slide gate chain and to look for an improved design, numerical simulations of simplified chain and cable models have been performed and compared. For the transient simulation of the strongly coupled system, a monolithic approach to fluid-structure interaction based on space-time finite elements has been used. Stability limits of 43 m/s and 60 m/s flow velocity have been detected for chain and cable model, respectively. Thus, by using a cable instead of a chain structure for slide gate operation, the situation may be improved, especially because a cable does not feature bolt connections which can be destroyed by strong vibrations. However, high amplitude flow induced vibrations cannot be prevented completely if the flow velocity in the slide gate duct reaches values up to 80 m/s.

6. REFERENCES

Hübner, B., Dinkler, D., 2005: A simultaneous solution procedure for strong interactions of generalized Newtonian fluids and viscoelastic solids at large strains. *International Journal for Numerical Methods in Engineering* 64, 920–939.

Hübner, B., Walhorn, E., Dinkler, D., 2004: A monolithic approach to fluid-structure interaction using space-time finite elements. *Computer Methods in Applied Mechanics and Engineering* 193, 2087–2104.

Païdoussis, M.P., Semler, C., 1998: Non-linear dynamics of a fluid-conveying cantilevered pipe with a small mass attached at the free end. *International Journal of Non-Linear Mechanics* 33, 15–32.